Article

pubs.acs.org/Biomac

Development of PLGA-Mannosamine Nanoparticles as Oral Protein Carriers

Maria Alonso-Sande,[†] Anne des Rieux,[‡] Virginie Fievez,[‡] Bruno Sarmento,[§] Araceli Delgado,[∥] Carmen Evora,[∥] Carmen Remuñán-López,[⊥] Véronique Préat,[‡] and Maria J. Alonso*[,†]

[†]CIMUS Research Institute, Campus Vida - University of Santiago de Compostela (USC), Spain

[‡]Louvain Drug Research Institute, Pharmaceutics and Drug Delivery Research Group, Université Catholique de Louvain, Belgium

[§]INEB - Instituto de Engenharia Biomédica, University of Porto, Portugal

[∥]Department of Chemical Engineering and Pharmaceutical Technology, University of La Laguna, Spain

[⊥]Nanobiofar Group, Department of Pharmacy and Pharmaceutical Technology, University of Santiago de Compostela, Spain

ABSTRACT: Here we report the development of polymeric nanoparticles, made of poly(lactide-*co*-glycolide) (PLGA) chemically modified with mannosamine (MN), intended to specifically interact with the intestinal mucosa and facilitate the intestinal transport of proteins. PLGA-MN nanoparticles displayed nanometric size and a negative zeta potential, which was lower than that of the PLGA nanoparticles. This correlate well with the preferential location of the MN group on the nanoparticles surface obtained by X-ray photoelectron spectroscope (XPS). The presence of MN groups in the polymer chain led to a different surface morphology noted by SEM, an increase of the encapsulation of model proteins, and to help stabilizing the nanoparticles in simulated intestinal fluids. Furthermore, the MN modification significantly enhanced the nanoparticle's interaction with the epithelial cells in human intestinal follicle-associated epithelium cell culture model. Overall, the MN modification significantly modifies the properties of PLGA nanoparticles making them more suitable as nanocarriers for oral protein delivery.

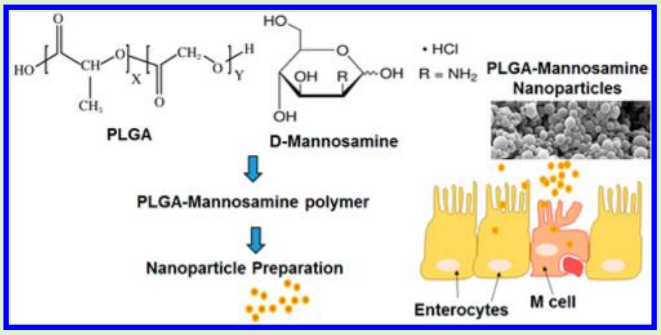

INTRODUCTION

Over the last decades, great efforts have been devoted to the design of new drug delivery systems, aimed at enhancing the absorption of drugs and vaccines across mucosal surfaces. Among them, polymeric nanoparticles have attracted significant attention due to their ability to interact with mucosal surfaces[1,2] and facilitate the transport of the associated macromolecules across them.[3,4]

Among them, poly(lactide-*co*-glycolide) (PLGA) nanoparticles are well-known because of their ability to associate and release proteins in a controlled manner.[5−7] Moreover, their potential as transmucosal carriers have been reported for both nasal and oral administration.[8,9] Nevertheless, these nanoparticles have certain disadvantages related to their instability in biological fluids and such as limited selectivity in their interaction with mucosal surfaces. In fact, a number of authors have already shown that PLA-based nanoparticles suffer an aggregation followed by degradation processes, which ultimately alter the drug stability and release.[10−12] An interesting approach aimed at solving the stability problem, has been the chemical modification of PLGA with PEG. The results from our group and others have shown that the PEG shell plays an interesting role improving the stability of the colloidal systems in biological fluids, and at improving their transport across different mucosal surfaces.[1,10−16] This improvement has been understood as a consequence of the nanoparticles stabilization process and their facilitated diffusion across the mucus.[17] However, PEG has not been found to directly influence the interaction with the underlying epithelium.

An alternative approach to enhance selectivity has been based upon the use of mannose as targeting ligand. Indeed, several authors have reported the enhancement of the interaction of mannose modified nanoparticles with specific cells in vitro and in vivo.[18−21] This higher cell uptake is related with the expression of mannose receptors by cells, such as macrophages and some epithelial cells in Peyer's Patches.[22,23] The mannose receptor is a transmembrane protein with five domains, able to specifically recognize mannose residues and frequently used to present antigens to the immune system.[24]

Taking this information into account, the aim of this work was to develop PLGA nanoparticles specifically targeted to the intestinal epithelium and, for this, we have chosen to chemically modify PLGA with mannosamine (MN) groups. The hypothesis behind was that the presence of mannose residues

Received: August 2, 2013
Revised: October 14, 2013
Published: October 16, 2013

on the particle surface could selectively target nanoparticles to M cells, increasing their affinity with the intestinal mucosa.

MATERIALS AND METHODS

Materials. PLGA 50:50, (Resomer 503, M_w 35 kDa), sodium cholate, albumin bovine (fraction V), bovine insulin and pancreatin from porcine pancreas, D-mannosamine hydrochloride, dicyclohexylcarbodiimide, dimethylaminopyridine, and rhodamine were purchased from Sigma Chemical (Madrid, Spain). Glucose and sucrose were obtained from Merck (Germany) and Probus (Spain), respectively. Dulbecco's modified Eagle's minimal essential medium (D-MEM, 25 mM glucose), RPMI 1640 medium, heat inactivated fetal calf serum, nonessential amino acids, L-glutamine, trypsin, PBS, Hank's balanced salt solution (HBSS), and penicillin-streptomycin (PEST) were purchased from Gibco Invitrogen Corporation (Carlsbad, CA). Human colon carcinoma Caco-2 line (clone 1) was obtained from Dr. Maria Rescigno, University of Milano-Bicocca, Milano, Italy. Human Burkitt's lymphoma Raji B line was supported by the American Type Culture collection (Manassas, VA). Ultrapure water (Milli-Q Plus, Millipore Ibérica, Spain) was used throughout.

Polymer Synthesis. The PLGA-mannosamine (PLGA-MN) was synthesized from PLGA (Resomer 503) of M_w of 34 kDa and MN 16 kDa determined by gel permeation chromatography. Terminal acid groups of PLGA were chemically modified with mannosamine in mild conditions and under nitrogen atmosphere.

Briefly, 17 mg of DMAP (dimethylaminopyridine) and 600 mg of PLGA were incorporated into 4 mL of stirred mannosamine solution in DMF (dimethylformamide; 6.87 mg/mL). Then, DCCI (dicyclohexylcarbodiimide) was added as coupling agent to start the reaction.[25] The mixture was kept under magnetic stirring at room temperature overnight. The product of the reaction was recovered by precipitation with deionized water. To purify, the polymer was dissolved in dichloromethane and precipitated with methanol and dried in desiccators under vacuum.

The reaction product was followed by ^{1}H NMR spectroscopy, using chloroform-d_1 as solvent. Control spectra were performed of mannosamine and original PLGA in deuterium oxide and chloroform-d_1, respectively.

Nanoparticle Preparation. PLGA and PLGA-MN nanoparticles were prepared by the double emulsion technique (w/o/w), as follows: 0.25 mg of BSA dissolved in 25 μL of water (10 mg/mL) or 1.25 mg of insulin in 125 μL of HCl 0.01 M (10 mg/mL) were emulsified in 0.5 mL solution of polymer in dichloromethane (50 mg/mL) by sonication (Branson 250 Sonifier) for 15 s (output 2). Then 2 mL of cholic acid solution (1% w/v) were added to this first emulsion and the resulting w/o/w emulsion was sonicated again for 15 s (output 2). The double emulsion was diluted rapidly in 25 mL of cholic acid solution (1% w/v), left on magnetic stirring for 10 min and then the solvent was eliminated to a final volume of 15 mL by evaporation under vacuum (Rotavapor R-114, Büchi, Switzerland).[5] Finally, the nanoparticles were isolated by centrifugation at 10000g for 30 min.

Unloaded and fluorescent nanoparticles (0.05 mg of rhodamine in ethanol) were obtained after one sonication step (o/w) in the same conditions as we described above.

Nanoparticle Characterization. Measurements of particle size, polydispersity, and zeta potential were performed by photon correlation spectroscopy (PCS) and laser doppler anemometry (LDA) using a Zetasizer III (Malvern Instruments; $n > 3$).

The morphological examination of nanoparticles was performed using the scanning electronic microscopy (SEM). For preparing the SEM samples 10 μL of the nanoparticle suspension were mounted onto metal stubs and dried for 48 h. The coating was performed with a gold alloy of 200- 300 Å thick. Superficial analyses of nanoparticles were carried out by X-ray photoelectron spectroscope (XPS) to confirm the localization of MN residues on the nanoparticle surface. XPS measurements were performed using a VG Escalab 250 iXL ESCA Instrument (VG Scientific), with a monochromatic Al−Kα radiation (hν = 1486.92 eV). Photoelectrons were collected from a take-off angle of 90° relative to the sample surface. The measurement was done in a constant analyzer energy mode with 100 eV pass energy for survey spectra and 20 eV pass energy for high resolution spectra. Surface elemental composition was determined using standard Scofield photoemission cross sections. The presence of O, C, and N was identified in the general spectra and the relative MN percentage was calculated based upon the atomic quantification of the identified components.

Freeze-Drying Process. Several concentrations of PLGA and PLGA-MN nanoparticles were frozen at −20 °C in the presence or absence of different concentrations of cryoprotector. Samples were then freeze-dried at 200 × 10^{-3} mBarr (Labconco, Kansas City, MI, United States), by following two steps: a primary drying step for 24 to 36 h at −30 °C, and a secondary drying step until the temperature gradually rose to +20 °C. PLGA and PLGA-MN nanoparticles were then resuspended in water and checked for particle size.

The investigated variables were the type and concentration of the cryoprotector and the nanoparticle concentration. First, we fixed the nanoparticle concentration at 0.5 mg/mL, and we varied the type of cryoprotector, glucose or sucrose, at two different concentrations 5 and 10%. Afterward, glucose 5% was selected as a cryoprotector and the final concentration of nanoparticles was 0.5, 1, or 2 mg/mL.

Stability of the Nanoparticles in Simulated Intestinal Medium (USP XXXVI). PLGA of PLGA-MN nanoparticles were incubated in simulated intestinal medium (USP XXXVI, pH 6.8, pancreatin 1% p/v) for 2 h at 37 °C. The particles interacting with biological components were separated by centrifugation at 1.000g for 2 min. The size and concentration of the remaining particles was determined by PCS and by measuring the optical absorbance in the supernatant (λ = 450 nm; UV-1603, UV-visible spectrophotometer Shimadzu). All samples were measured against a blank solution of simulated intestinal medium[14] ($n > 4$).

Protein Encapsulation. BSA and insulin were chosen as model proteins to evaluate the effect of MN modification on the ability of nanoparticles to encapsulate therapeutic proteins. The amount of BSA and insulin entrapped in nanoparticles was calculated by the difference between the theoretical content and the amount of free protein found in the supernatant, measured by the microBCA protein assay (λ = 570 nm). Calibration curve were made using supernatants of the corresponding unloaded nanoparticles ($n = 6$).

Protein encapsulation efficiency (EE) of nanoparticles was calculated as indicated below:

$$\mathrm{EE}(\%) = \frac{\text{total amount of protein} - \text{free protein}}{\text{total amount of protein}} \times 100\%$$

Protein Release. The release of BSA and insulin from PLGA or PLGA-MN nanoparticles was investigated by incubation of particles in PBS (pH 7.4) for 28 days at 37 °C. At appropriate intervals (1 h, 1 day, 3 days, 7 days, 14 days, and 28 days) the samples were collected and centrifuged at 22000g for 30 min. The protein concentration in the release medium was determined by the micro BCA protein assay (λ = 570 nm). A calibration curve was made at each time interval using nonloaded nanoparticles ($n = 9$).

Cell Culture Experiments. In vitro cell culture studies were carried out on Caco-2 cell monocultures and Caco-2 and Raji cells cocultures. Caco-2 cells (human colon carcinoma, clone1) and Raji cells were cultivated on flasks using supplemented D-MEM and RPMI medium. Caco-2 cells were passed to achieve 90% confluence (4−5 days). Raji cells were passed every 8−9 days by three times dilution. The media were changed every other day 26. The passage used for experiments varied between 19 and 34 and 109−119 for Caco-2 and Raji cells, respectively.

In Vitro Quantitative Transport and Uptake Studies. Caco-2 cells were seeded with a density of 5 × 10^5 cells per well in 12-well plates (membrane pore diameter of 3 μm, Corning Costar, New York, NY) over a basement membrane Matrix (Matrigel TM, Becton Dickinson, Bedford, MA) using D-MEM medium supplemented with 10% fetal calf serum, 1% of L-glutamine (v/v), 1% (v/v) of PEST, and 1% (v/v) of nonessential amino acids. After three days of incubation, the inserts were inverted and placed in Petri dishes, and sterile silicon

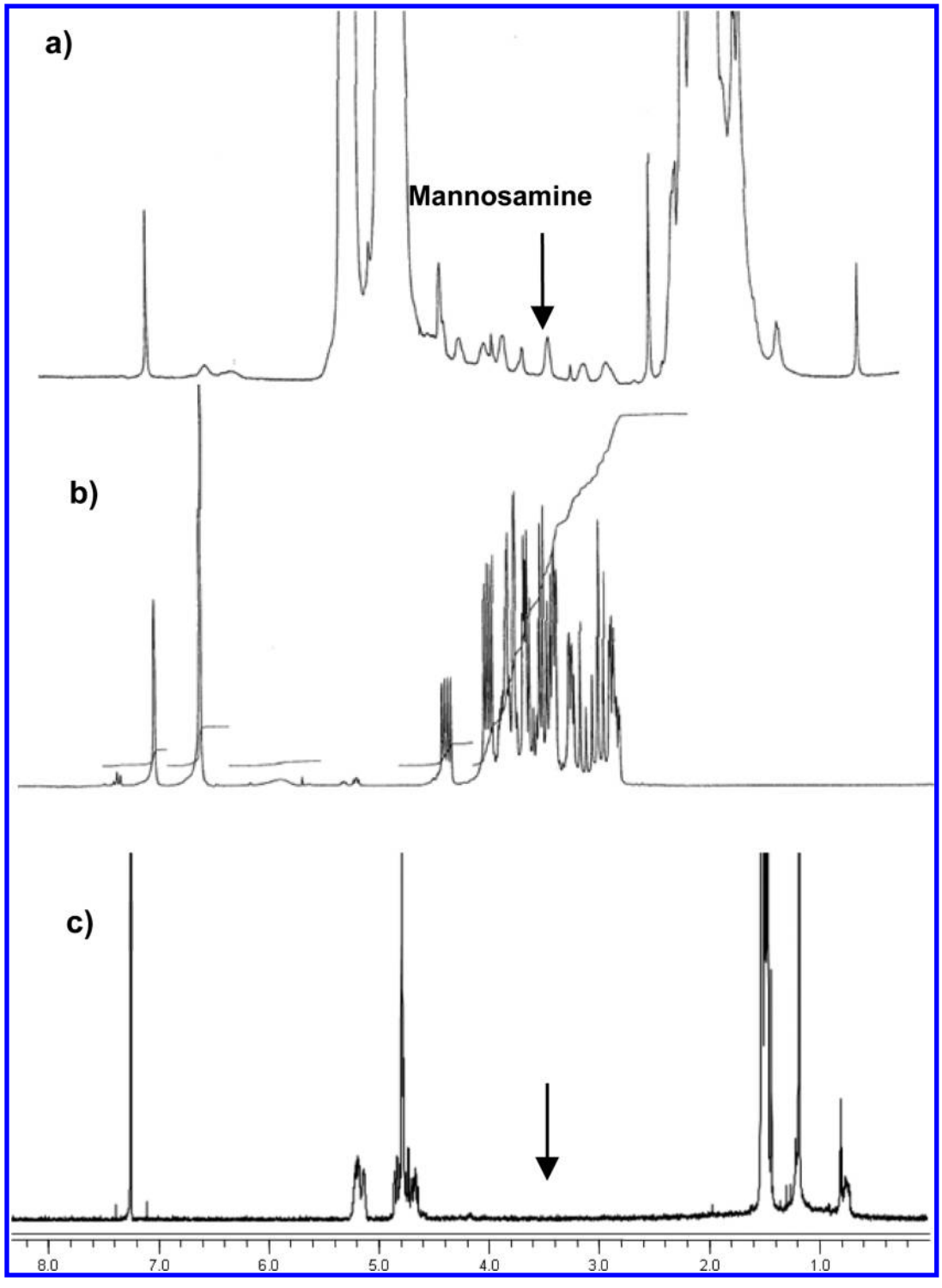

Figure 1. NMR spectra corresponding to PLGA-MN (a), MN (b), and PLGA polymer (c).

tubes were placed around the basolateral sides of the inserts. A total of 14 days later, Raji cells were added in the basolateral compartments. Cocultures were maintained for 5 days. Monocultures of Caco-2 cells, cultivated as above, except for the presence of Raji cells, were used as controls.

Prior to starting experiments, silicon tubes were removed; cell monolayers were placed in new multiwell plates.[26] Culture medium of mono- and cocultures was removed and substituted by HBSS. Then, transepithelial electric resistance (TEER) values were measured with an Endohm tissue resistance chamber (Endohm-12, World Precision Instruments, Sarasota, FL) to verify the integrity of the cell monolayer and the conversion of enterocytes to M cells. The TEER values were around 300 and 150 $\Omega \cdot cm^2$ for monocultures and cocultures, respectively. Afterward, cell monolayers were incubated with fluorescent nanoparticles (1 mg/mL, 2×10^8 nanoparticles/mL) in HBSS for 90 min under different conditions.

Following each experiment, basolateral solutions were analyzed by flow cytometry (FACScan, Becton Dickinson) to measure the number of transported nanoparticles. Although no control assays were performed in order to confirm the nanoparticle integrity, this approach has been well referenced before to evaluate the transport of PLGA nanoparticles, demonstrating its consistency.[26−28] Next, the cell

Table 1. Physicochemical Characterization of Isolated PLGA and PLGA-MN Nanoparticles

polymer	size (nm)	polydispersity	potential zeta (mV)	MN content (%)
PLGA	276.0 ± 27.3	0.209 ± 0.080	−55.1 ± 1.8	0
PLGA-MN	246.4 ± 13.5	0.251 ± 0.038	−43.3 ± 3.4[a]	0.115 ± 0.024

[a]Statistical differences $P < 0.05$ (mean ± SD, $n = 6$).

monolayers were rinsed five times with cold PBS (pH = 5) in order to remove the particles that were not strongly associated with the cells, and incubated with an "acid wash" solution (EDTA 5 mM in PBS, pH = 5) for 15 min. Finally, the monolayers were dried overnight and dissolved in a "Lysis Medium" (2% SDS/50 mM EDTA in PBS, pH = 6). The number of strongly associated nanoparticles was quantified by flow cytometry (FACScan, Becton Dickinson). The results were expressed as percentage of the donor solution ($n > 3$).

Statistical Analysis. The statistical significance was studied by the ANOVA One-Way test (SigmaStat Program, Jandel Scientific, version 2.0). Differences were considered to be significant at a level of $P < 0.05$.

RESULTS AND DISCUSSION

This work aimed at evaluating the potential benefit of PLGA chemical modification with MN in the performance of the resulting nanoparticles as carriers for oral protein administration. More specifically, the influence of the polymer modification was studied with regard to its influence on (i) nanoparticles stability in intestinal fluids; (ii) protein loading and release capacity; and (iii) interaction with the FAE model cell line epithelium.

Mannosamine Modification of PLGA. The success on the chemical modification of PLGA was confirmed by ^{1}H NMR. In Figure 1 is depicted the ^{1}H NMR spectra corresponding to PLGA-MN, MN, and PLGA polymer. From their comparison, we observed that the signals between 3 and 4 ppm (ppm) in PLGA-MN polymer (Figure 1a) were no present in original PLGA spectrum (Figure 1c) and their localization in the PLGA-MN spectrum match with MN peaks (Figure 1b). Additionally, the broadening and the displacement of these signals in PLGA-MN polymer spectrum (Figure 1a) could be explained by the change in the chemical environment of MN.

MN Groups are Present on the Surface of MN-PLGA Nanoparticles. The physicochemical properties of unloaded PLGA and PLGA-MN nanoparticles, prepared by the simple emulsion method, are summarized in Table 1. The MN attachment to PLGA did not cause a significant change of the particle size or polydispersity. However, PLGA-MN nanoparticles exhibited a zeta potential that was significantly lower than that of PLGA nanoparticles. This modification led us to speculate about the localization of MN residues on the nanoparticle's surface as it was previously reported by others authors for hydrophilic modifications of PLGA polymer.[10,16] This hypothesis was additionally supported by the wrinkled surface (Figure 2) of PLGA-MN nanoparticles as compared to the smooth surface of PLGA nanoparticles observed by SEM.

According to the XPS surface analysis of nanoparticles, the oxygen content onto the surface of PLGA-MN nanoparticles doubled the one corresponding to PLGA nanoparticles (0.31 vs 0.17; Table 2). Furthermore, the percentage of nitrogen residues (w/w), which can be only related with MN moieties, on the nanoparticles surface was around 0.11%, a value that is close to the theoretical MN content in the original polymer. Moreover, the external aqueous phase favors the superficial orientation of hydrophilic residues such as MN. These results

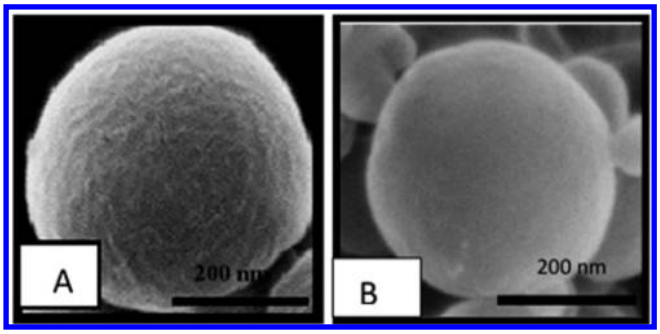

Figure 2. SEM photographs of PLGA-MN (A) and PLGA (B) nanoparticles.

Table 2. Atomic Composition of PLGA and PLGA-MN Surface

formulation	C %	O %	O/C ratio
PLGA	79.1	16.9	0.21
PLGA-MN	63.6	31.4	0.49

agree with those reported by Kim and co-workers, where significant changes of the superficial composition of coated PLGA nanoparticles were detected by XPS.[27] Consequently, this result, together with previous changes in zeta potential depicted in Table 1, could be taken as an indication of the preferential surface localization of the MN residues.

MN-PLGA Nanoparticles Can Be Freeze-Dried and Reconstituted. From the pharmaceutical point of view, the conversion of the PLGA nanoparticle suspensions into powders is critical in order to avoid particle degradation during storage. To assess the feasibility of the freeze-drying of MN-modified nanoparticles, two different sugars, glucose and sucrose, were used (Figure 3a). The sugar concentration was of 5 and 10% w/v, and the nanoparticle concentration was in the range of 0.5 to 2 mg/mL (Figure 3b). The results indicated that, as in the case of PLGA nanoparticles, the presence of a cryoprotector is essential for the adequate reconstitution of PLGA-MN nanoparticles upon freeze-drying process. However, the type or the concentration of the cryoprotector did not have a significant influence on the final size of the reconstituted nanoparticles (Figure 3a).[28] On the other hand, the results in Figure 3b revealed that the freeze-dried nanoparticles can be conveniently resuspended, irrespective of their initial concentration (0.5, 1, and 2 mg/mL). Overall, the modification of the polymer with MN did not affect the feasibility of the freeze-drying process.

MN Groups Enhance the Stability of MN-PLGA Nanoparticles in Simulated Intestinal Medium (USP XXXVI). As the surface modification of PLGA nanoparticles may influence their stability in intestinal fluids,[10,11] we hypothesized that the MN residues in the nanoparticles surface could increase their stability. Thus, we incubated the nanoparticles in intestinal medium with pancreatin (USP XXXVI) for 2 h and determined the percentage that remained in suspension and their size. In agreement with previous reports

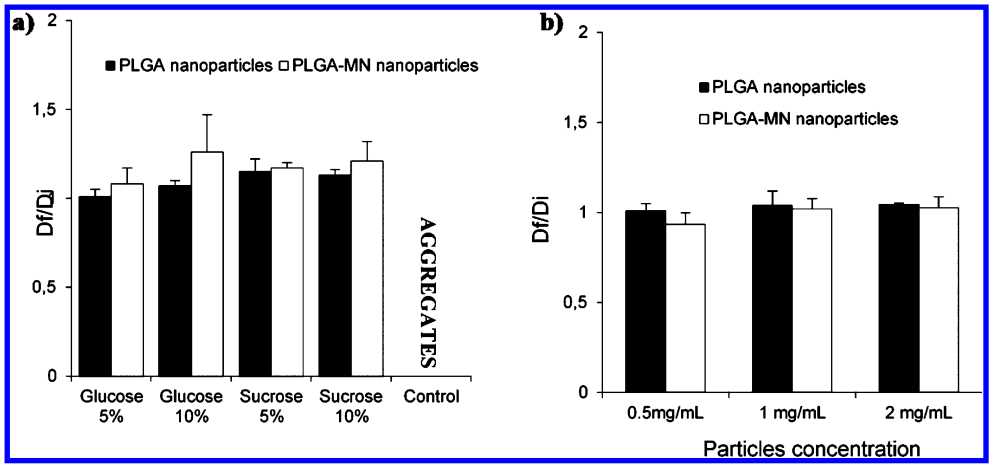

Figure 3. Effect of the type and concentration of the cryoprotector (a) and of the particle concentration (freeze-dried with glucose 5%; b) on the size of PLGA and PLGA-MN nanoparticles after freeze-drying process. Df: mean particle size after freeze-drying and further resuspension. Di: mean initial particle size (mean ± SD, n = 4).

on the effect of intestinal enzymes in nanoparticle aggregation,[10−12] the results showed that both PLGA and MN-PLGA nanoparticles undergo a certain aggregation upon incubation with the intestinal fluid. However, the presence of MN on the nanoparticles surface led to some improvement in their stability (table 3). In fact, after 2 h of incubation the percentage of PLGA-MN nanoparticles remaining in suspension was higher (49% vs 35%) and their size was smaller (398 vs 512 nm) than that of PLGA nanoparticles. This stabilizing effect of MN was similar to the one observed for PEGylated nanoparticles,[10] suggesting the potential protein repellent effect of the MN residues.

Table 3. Interaction of PLGA and PLGA-MN Nanoparticles with Simulated Intestinal Fluid Compounds after Incubation by 2 h at 37 °C (Mean ± SD, $n \geq 3$)

polymer	time (h)	size (nm)	remaining particles (%)
PLGA	0	266 ± 13	100
	1	357 ± 23	50 ± 14
	2	512 ± 68	35 ± 5
PLGA-MN	0	284 ± 18	100
	1	337 ± 17	59 ± 6
	2	398 ± 56	49 ± 6

MN Groups Enhance the Protein Encapsulation Efficacy of MN-PLGA Nanoparticles. Two different model proteins, BSA (M_w: 69 kDa, IP: 4.7) and insulin (M_w: 5.8 kDa, IP: 5.3), were selected as model compounds in order to investigate the influence of the MN modification on the ability of PLGA nanoparticles to associate hydrophilic proteins. The results depicted in Table 4 indicated that both PLGA and PLGA-MN nanoparticles, prepared by double emulsion method, presented high protein encapsulation efficiencies. However, the presence of MN residues in the polymer chain, led to a 10% enhancement in the encapsulation efficiency of both proteins. This could be explained by the interaction between proteins and the mannose residues in polymer. Sugimoto and co-workers reported that saccharides show diverse mechanisms of protein recognition, and most of them involve hydrogen and van der Waals bonding.[29] Hence, saccharide modification could lead to a more hydrophilic polymer, with higher affinity for proteins.

Table 4. Encapsulation Efficacies of PLGA and PLGA-MN Nanoparticles[a]

polymer	insulin encapsulation efficiency (%)	BSA encapsulation efficiency (%)
PLGA	68 ± 2	68 ± 1
PLGA-MN	77 ± 15	84 ± 2

[a]Insulin theoretical loading 5%, BSA theoretical loading 1% (mean ± SD, n = 6).

MN Groups Do Not Affect Protein Release from MN-PLGA Nanoparticles. Given the influence of the MN groups of the protein encapsulation, it could be expected that they would also affect the protein release rate. Nevertheless, the results in Figure 4 indicate that such modification did not have an impact on the release of the encapsulated protein. This could be explained by the fact that the drug release rate from PLGA nanoparticles is mainly governed by the degradation of the polymer matrix,[30] which might not be affected by the presence of MN.

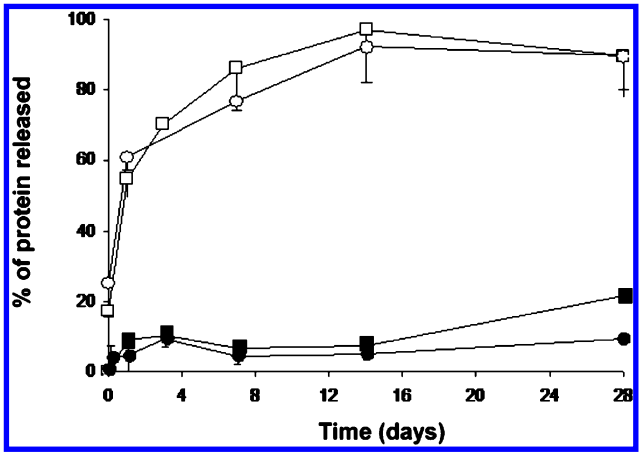

Figure 4. In vitro protein release profiles from PLGA (circles) and PLGA-MN (squares) nanoparticles after 28 days in PBS (pH 7.4) at 37 °C. Open symbols: percentages of BSA released. Close symbols: percentages of insulin released (mean ± SD, n = 9).

However, a different profile was obtained for the two model proteins investigated. More specifically, most of the encapsu-

dx.doi.org/10.1021/bm401141u | Biomacromolecules 2013, 14, 4046−4052

lated of BSA was released from nanoparticles in a few days, whereas, the amount of insulin released along the study was less than 20%. This finding could be attributed to the different distribution of the entrapped proteins into the polymer matrix as a consequence of their different size BSA M_w: 69 kDa, insulin M_w: 5.8 kDa. Moreover, we cannot discard the possibility of the interaction of the encapsulated insulin with the polymer degradation products or even its degradation in the acidic environment as previously reported.[31] Although these results cannot be extrapolated to the in vivo situation, we could conclude that the MN modification of PLGA did not affect the in vitro release profile and that additional efforts might be needed in order to further control the release of insulin from PLGA-MN nanoparticles.

MN Groups Enhance the Affinity of MN-PLGA Nanoparticles for M Cells. To study the mechanisms involved in the interactions of these nanoparticles across the intestinal mucosa, rhodamine-loaded PLGA, and PLGA-MN nanoparticles were incubated with mono- and cocultures, as in vitro models for normal enterocytes and M cells, respectively. Nanoparticles were incubated with the cell monolayers for 90 min, at different conditions. Then, the basolateral media and cell lysates were sampled to quantify the amount of fluorescent nanoparticles that were associated to the monolayer.

From the analysis of the basolateral media, it was deduced that the transport of MN-PLGA nanoparticles across the coculture was 2-fold higher than for the monoculture (results not shown). In addition, it was found that, despite the limited transport in both, mono-, and cocultures, the amount of nanoparticles crossing the monolayer was higher for MN-PLGA nanoparticles than for PLGA nanoparticles (0.011 vs 0.111% of donor solution in monoculture and 0.022 vs 0.193% of donor solution in coculture for PLGA and PLGA-MN nanoparticles, respectively). This result suggest the potential of MN residues as ligand to improve the affinity of PLGA nanoparticles by nonspecific and specific interactions with both enterocytes and M cells. Moreover, the incubation of nanoparticles with both monolayers at 4 °C decrease the transport of nanoparticles more than 3-fold (data not shown) in comparison with the results obtained at 37 °C. These findings agree with earlier results reported by Fievez and co-workers, where MN residues improved the transport of PLGA-PCL-PEG nanoparticles through FAE model.[32]

Cells lysates were also analyzed to quantify the amount of nanoparticles internalized by the cells or strongly associated to them. As shown in Figure 5, the interaction of PLGA-MN nanoparticles with the FAE monolayer was significantly higher than that of the PLGA ones, reaching values as high as 20%. As expected, this result could be attributed to the positive role of MN residues in enhancing the interaction of PLGA-MN nanoparticles with M-cells (~10−20%). These results reveal the higher affinity of MN-PLGA nanoparticles by M cells as compared to that of PLGA nanoparticles. The greater transport described above for MN-PLGA nanoparticles in regular Caco-2 cells as compared to PLGA nanoparticles can not be explained in terms of greater uptake but probably in terms of their enhanced stability. However, this is only a speculation as the amount of nanoparticles crossing the epithelium is indeed low. Moreover, uptake experiments performed at 4 °C, showed a significant reduction of the number of nanoparticles associated to monolayers, indicating that the uptake of MN-PLGA nanoparticles is an active mechanism (data not shown), probably involving the formation of endosomes.[33]

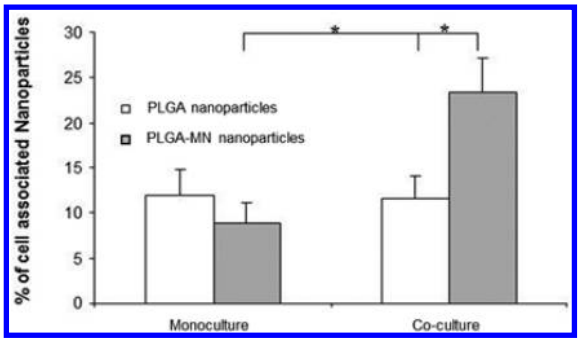

Figure 5. Influence of MN modification on the nanoparticle uptake. Percentage of PLGA and PLGA-MN nanoparticles strongly associated to the cells following 90 min of incubation at 37 °C, comparing monocultures and cocultures. *Significant differences ($P < 0.05$; mean ± SEM, $n = 6$).

All of these results suggest that these nanoparticles interact with M cells via receptor-mediated endocytosis. However, up to date, no identification of mannose receptor has been confirmed in this in vitro model. Therefore, more detailed experiments should be done in order to clarify the mechanisms involving mannosylated nanoparticle uptake, as well as to confirm their affinity by specific receptors overexpressed in human M cells. Beyond these mechanistic details, the enhancement of the affinity of MN-modified nanoparticles by M cells, points out their potential as carriers for systemic protein delivery and, notable, for their delivery to the immune system.

■ CONCLUSIONS

We have developed a new protein carrier made of chemically modified PLGA polymer with MN. The decrease of zeta potential values, the significant changes of the superficial composition detected by XPS together with the wrinkled surface observed on the PLGA-MN nanoparticles suggests that the MN could be located on the particle surface. Mannose modification improved the particle stability in simulated intestinal medium, as well as the association of hydrophilic proteins, such as insulin and BSA, allowing a higher nanoparticle uptake, and suggesting a better interaction with the intestinal epithelium.

■ AUTHOR INFORMATION

Corresponding Author

*Phone: +34 881815454/+34 981594488, ext. 15454. E-mail: mariaj.alonso@usc.es.

Notes

The authors declare no competing financial interest.

■ ACKNOWLEDGMENTS

The authors would like to thank the Ministry of Education (Consolider Ingenio 2010, CSD2006-00012), the Xunta de Galicia (Competitive Reference Groups), the Spanish Ministry of Economy and Competitivity (SAF2011-30337-C02-02) and the Région Wallonne (VACCINOR) and FRSM (Belgium) for the financial support of some of the work included in this paper. M.A.S. acknowledges the Spanish Government her Predoctoral grant (FPU-MEC).

■ REFERENCES

(1) Vila, A.; Gill, H.; McCallion, O.; Alonso, M. J. *J. Controlled Release* **2004**, *98*, 231−244.

(2) Primard, C.; Rochereau, N. E.; Genin, C.; Delair, T.; Paul, S.; Verrier, B. *Biomaterials* **2010**, *31*, 6060−6068.
(3) García-Fuentes, M.; Alonso, M. J. *J. Controlled Release* **2012**, *161*, 496−504.
(4) des Rieux, A.; Pourcelle, V.; Cani, P. D.; Marchand-Brynaert, J.; Preat, V. *Adv. Drug Delivery Rev.* **2013**, *65*, 833−844.
(5) Blanco, M. D.; Alonso, M. J. *Eur. J. Pharm. Biopharm.* **1997**, *43*, 287−294.
(6) Parajó, Y.; D'Angelo, I.; Horváth, A.; Vantus, T.; György, K.; Welle, A.; Garcia-Fuentes, M.; Alonso, M. J. *Eur. J. Pharm. Sci.* **2010**, *41*, 644−649.
(7) Kumari, A.; Yadav, S. K.; Yadav, S. C. *Colloids Surf., B* **2010**, *75*, 1−18.
(8) Mittal, G.; Carswell, H.; Brett, R.; Currie, S.; Ravi Kumar, M. N. V. *J. Controlled Release* **2011**, *150*, 220−228.
(9) Sarti, F.; Perera, G.; Hintzen, F.; Kotti, K.; Karageorgiou, V.; Kammona, O.; Kiparissides, C.; Bernkop-Schnürch, A. *Biomaterials* **2011**, *32*, 4052−4057.
(10) Tobio, M.; Sanchez, A.; Vila, A.; Soriano, I.; Evora, C.; Vila-Jato, J. L.; Alonso, M. J. *Colloids Surf., B* **2000**, *18*, 315−323.
(11) Bazile, D.; Prud'homme, C.; Bassoullet, M. T.; Marlard, M.; Spenlehauer, G.; Veillard, M. *J. Pharm. Sci.* **1995**, *84*, 493−498.
(12) Reix, N.; Parat, A.; Seyfritz, E.; Van Der Werf, R.; Epure, V.; Ebel, N.; Danicher, L.; Marchioni, E.; Jeandidier, N.; Pinget, M.; Frère, Y.; Sigrist, S. *Int. J. Pharm.* **2012**, *437*, 213−220.
(13) De Campos, A.; Sánchez, A.; Gref, R.; Calvo, P.; Alonso, M. J. *Eur. J. Pharm. Sci.* **2003**, *20*, 73−81.
(14) Tobio, M.; Gref, R.; Sanchez, A.; Langer, R.; Alonso, M. J. *Pharm. Res.* **1998**, *15*, 270−275.
(15) Vila, A.; Sanchez, A.; Tobío, M.; Calvo, P.; Alonso, M. J. *J. Controlled Release* **2002**, *78*, 15−24.
(16) Avgoustakis, K.; Beletsi, A.; Panagi, Z.; Klepetsanis, P.; Livaniou, E.; Evangelatos, G.; Ithakissios, D. S. *Int. J. Pharm.* **2003**, *259*, 115−127.
(17) Ensign, L. M.; Cone, R.; Hanes, J. *Adv. Drug Delivery Rev.* **2012**, *64*, 557−570.
(18) Cui, Z.; Hsu, C.-H.; Mumper, R. J. *Drug Dev. Ind. Pharm.* **2003**, *6*, 689−700.
(19) Hashimoto, M.; Morimoto, M.; Saimoto, H.; Shigemasa, Y.; Yanagie, H.; Eriguchi, M.; Sato, T. *Biotechnol. Lett.* **2006**, *28*, 815−821.
(20) Tomizawa, H.; Aramaki, Y.; Fujii, Y.; Hara, T.; Suzuki, N.; Yachi, K.; Kikuchi, H.; Tsuchiya, S. *Pharm. Res.* **1993**, *4*, 549−552.
(21) Takada, M.; Yuzurita, T.; Katayama, K.; Iwamoto, K.; Sunamoto, J. *Biochim. Biophys. Acta* **1984**, *802*, 237−244.
(22) Linehan, S. A.; Martínez-Pomares, L.; Stahl, P. D.; Gordon, S. *J. Exp. Med.* **1999**, *189*, 1961−1972.
(23) Linehan, S. A.; Martínez-Pomares, L.; da Silva, R. P.; Gordon, S. *Eur. J. Immunol.* **2001**, *31*, 1857−1866.
(24) Stahl, P. D.; Schulesinger, P. H.; Singardson, E.; Rodman, J. S.; Lee, Y. C. *Cell* **1980**, *19*, 207−215.
(25) Sheehan, J. C.; Hess, G. P. *J. Am. Chem. Soc.* **1955**, *77*, 1067−1068.
(26) des Rieux, A.; Theat, I.; Fievez, V.; Préat, V.; Schneider, Y. J. *Eur. J. Pharm. Sci.* **2007**, *30*, 380−391.
(27) Kim, S. H.; Jeong, J. H.; Chun, K. W.; Park, T. G. *Langmuir* **2005**, *21*, 8852−8857.
(28) Jeong, Y. I.; Shim, Y. H.; Kim, C.; Lim, G. T.; Choi, K. C.; Yoon, C. *J. Microencapsulation* **2005**, *22*, 593−601.
(29) Sugimoto, N.; Miyoshi, D.; Zou, J. *Chem. Commun.* **2000**, 2295−2296.
(30) Belbella, A.; Vauthier, C.; Fessi, H.; Devissaguet, J.; Puisieux, F. *Int. J. Pharm.* **1996**, *129*, 95−102.
(31) Bilati, U.; Allémann, E.; Doelker, E. *Eur. J. Pharm. Biopharm.* **2005**, *59*, 375−388.
(32) Fievez, V.; Plapied, L.; des Rieux, A.; Pourcelle, V.; Freichels, H.; Wascotte, V.; Vanderhaeghen, M. L.; Jerôme, C.; Vanderplasschen, A.; Marchand-Brynaert, J.; Schneider, Y. J.; Préat, V. *Eur. J. Pharm. Biopharm.* **2009**, *73*, 16−24.
(33) Desai, M. P.; Labhasetwar, V.; Walter, E.; Levy, R. J.; Amidon, G. L. *Pharm. Res.* **1997**, *14*, 1568−1573.